

A novel glycosylated anti-CD20 monoclonal antibody from transgenic cattle

Ran Zhang¹, Chenjun Tang¹, Huaizu Guo², Bo Tang³, Sheng Hou², Lei Zhao⁴, Jianwu Wang³, Fangrong Ding¹, Jianmin Zhao³, Haiping Wang¹, Zhongzhou Chen¹, Yunping Dai^{1*}, Ning Li^{1*}

¹State Key Laboratory for Agrobiotechnology, College of Biological Sciences, China Agricultural University, Beijing 100194, China

²State Key Laboratory of Antibody Medicine and Targeted Therapy, Shanghai Key Laboratory of Cell Engineering; Shanghai 200433, China

³Wuxi KGBIO biotechnology Limited Liability Company, Wuxi 214145, China

⁴ National Clinical Research Center for Normal Aging and Geriatric, Institute of Geriatric, PLA General Hospital, Beijing 100853, China

Correspondence and requests for materials should be addressed to Y.D. (email: daiyunping@sina.com) or N.L. (email: ninglcau@126.com)

Figure S1 Verification of transgene integration. (a) Image of transgenic cattle expressing the recombinant anti-CD20 mAb at the farm. (b) PCR detection of the integration sites. The product for the wild-type sequence was 671 bp, whereas the product for the 3' flanking region of the transgenic sequence was 405 bp. (c, d) Detection of the transgene location in the transgenic cattle by the GTG-binding pattern of metaphase spreads before hybridization (c) and the same metaphase spreads after FISH (d). The arrows indicate the transgene integration site in chromosome 3.

Figure S2 Verification of the transgene genetic stability of transgenic offspring. (a) PCR detection of the transgenes in transgenic offspring. Marker, 1-kb DNA ladder; P-LC, positive plasmid containing the LC-encoding sequences; P-HC, positive plasmid containing the HC-encoding sequences; WT, genomic DNA of wild-type cattle; genomic DNA of transgenic cattle indicated by 1321, 1325 and 0220. The amplified products for the HC- or LC-encoding sequences were 1.5 kb and 0.8 kb, respectively. (b, c) Expression of the recombinant anti-CD20 mAb in the milk of transgenic offspring, as characterized by SDS-PAGE (b) and western blotting under reducing conditions (c). WT, milk from wild-type cattle. PC, purified human IgG.

Figure S3 Peptide mapping of the HC of the recombinant anti-CD20 mAb and Rituxan. Peptide sequences highlighted in red indicate the allotype of the recombinant mAb. The dashes represent amino acids that are identical to those of Rituxan.

Figure S4 SPR analysis of the binding affinity of the recombinant anti-CD20 mAb to human Fc γ RIIIa. The sensorgrams obtained for the surface blank and buffer blank control were subtracted from the sensorgrams obtained for the antibodies to yield the

curves shown here. (a, b) Interaction between the recombinant anti-CD20 mAb and Fc γ RIIIa-Phe158 (a) or Fc γ RIIIa-Val158 (b). The concentrations of the recombinant anti-CD20 mAb are 3.333, 10, 30, 90, 270, and 810 nM, as indicated. (c, d) Interaction between Rituxan and Fc γ RIIIa-Phe158 (c) or Fc γ RIIIa-Val158 (d). The concentrations of Rituxan are 30, 90, 270, 810, 2430, 7,290, and 21,870 nM, as indicated.

Table S1. The whole N-glycan profiles of recombinant anti-CD20 mAb.

Milk mAb							
RT (min)	Short name	Composition	Structura scheme	Expected mass (Da)	Observed mass (Da)	Δmass (ppm)	FLR Area%
15.09	G0-GlcNAc	Hex3HexNAc3	 A branched N-glycan structure consisting of a core glucose (green circle) attached to three N-acetylglucosamine (blue squares) units. One branch contains two N-acetylglucosamine units, and the other contains one.	1234.4832	1234.478	-4.21	0.13
18.56	G0	Hex3HexNAc4	 A branched N-glycan structure consisting of a core glucose (green circle) attached to three N-acetylglucosamine (blue squares) units. One branch contains two N-acetylglucosamine units, and the other contains one. An additional N-acetylglucosamine unit is attached to the side chain of one of the terminal N-acetylglucosamine units.	1437.5625	1437.558	-3.13	0.53
18.83	/	Hex5HexNAc2	/	1355.5095	1355.234	-203.29	0.19
20.52	G1-GlcNAc	Hex4HexNAc4	 A branched N-glycan structure consisting of a core glucose (yellow circle) attached to four N-acetylglucosamine (blue squares) units. One branch contains two N-acetylglucosamine units, and the other contains one.	1396.5360	1396.537	0.72	0.94
21.00	G0F	Hex3HexNAc4 DHex1	 A branched N-glycan structure consisting of a core glucose (green circle) attached to three N-acetylglucosamine (blue squares) units. One branch contains two N-acetylglucosamine units, and the other contains one. An additional N-acetylglucosamine unit is attached to the side chain of one of the terminal N-acetylglucosamine units, and a fucose (red triangle) is attached to the side chain of another.	1583.6205	1583.618	-1.58	0.57
22.27	Man5	Hex5HexNAc2	 A branched N-glycan structure consisting of a core glucose (green circle) attached to five N-acetylglucosamine (blue squares) units. One branch contains two N-acetylglucosamine units, and the other contains one.	1355.5095	1355.496	-9.96	7.89
23.09	G1	Hex4HexNAc4	 A branched N-glycan structure consisting of a core glucose (yellow circle) attached to four N-acetylglucosamine (blue squares) units. One branch contains two N-acetylglucosamine units, and the other contains one.	1599.6154	1599.608	-4.63	2.71
23.39		Hex4HexNAc4		1599.6154	1599.603	-7.75	0.54
23.70		Hex4HexNAc4		1599.6154	1599.609	3.98	0.68
25.17	Man5Gn	Hex5HexNAc3	 A branched N-glycan structure consisting of a core glucose (green circle) attached to five N-acetylglucosamine (blue squares) units. One branch contains two N-acetylglucosamine units, and the other contains one. A fucose (red triangle) is attached to the side chain of one of the terminal N-acetylglucosamine units.	1558.5888	1558.581	5.02	3.96
26.01	G1F	Hex4HexNAc4 DHex1	 A branched N-glycan structure consisting of a core glucose (yellow circle) attached to four N-acetylglucosamine (blue squares) units. One branch contains two N-acetylglucosamine units, and the other contains one. An additional N-acetylglucosamine unit is attached to the side chain of one of the terminal N-acetylglucosamine units, and a fucose (red triangle) is attached to the side chain of another.	1745.6733	1745.664	-5.33	1.28
26.28	/	Hex4HexNAc5	 A branched N-glycan structure consisting of a core glucose (yellow circle) attached to four N-acetylglucosamine (blue squares) units. One branch contains two N-acetylglucosamine units, and the other contains one. An additional N-acetylglucosamine unit is attached to the side chain of one of the terminal N-acetylglucosamine units, and a fucose (yellow square) is attached to the side chain of another.	1802.6947	1802.703	-4.58	0.38

Milk mAb							
RT (min)	Short name	Composition	Structura scheme	Expected mass (Da)	Observed mass (Da)	Δmass (ppm)	FLR Area%
26.91	Man6	Hex6HexNAc2		1517.5623	1517.573	7.05	6.72
27.29		Hex6HexNAc2		1517.5623	1517.547	-10.08	2.33
27.97	G2	Hex5HexNAc4		1761.6682	1761.662	-3.52	36.04
29.07	/	Hex6HexNAc3	/	1720.6416	1720.651	-5.44	1.66
29.99	G2F	Hex5HexNAc4 DHex1		1907.7261	1907.703	-12.11	12.95
30.87	/	Hex5HexNAc3 NANA		1849.6842	1849.767	-44.74	1.69
31.31	Man7	Hex7HexNAc2		1679.6151	1679.689	44.00	3.13
31.63		Hex7HexNAc2		1679.6151	1679.685	41.61	1.02
32.02		Hex7HexNAc2		1679.6151	1679.672	33.88	1.30
32.92	G2+NeuAc1	Hex5HexNAc4 NeuAc1		2052.7636	2052.782	8.96	0.90
33.35	/	Hex7HexNAc3	/	1882.6954	1882.689	2.91	1.41
34.13	/	Hex6HexNAc3Ne uAc1		2011.7371	2011.719	-9.00	1.71
34.75				2011.7371	2011.724	6.49	1.95

Milk mAb							
RT (min)	Short name	Composition	Structura scheme	Expected mass (Da)	Observed mass (Da)	Δmass (ppm)	FLR Area%
35.59	Man8	Hex8HexNAc2	A branched glycan structure consisting of a core glucose unit (green) with two terminal sialic acid units (blue) and three internal galactose units (yellow). The structure is highly branched with multiple linkage points.	1841.6679	1841.660	-4.29	4.82
36.09	/	Hex6HexNAc4Ne uAc1	A branched glycan structure consisting of a core glucose unit (green) with one terminal sialic acid unit (blue), four internal galactose units (yellow), and one acetyl group (pink). The structure is highly branched with multiple linkage points.	2214.8164	2214.794	-10.11	0.29
36.56				2214.8164	2214.805	-5.15	0.27

Table S2. The whole N-glycan profiles of Rituxan.

Rituxan							
RT (min)	Short name	Composition	Structura scheme	Expected mass (Da)	Observed mass (Da)	Δmass (ppm)	FLR Area%
18.33	G0F-GlcNAc	Hex3HexNAc3 DHex1		1380.5411	1380.548	5.00	0.79
19.07	G0	Hex3HexNAc4		1437.5625	1437.549	-9.39	1.00
21.50	G0F	Hex3HexNAc4 DHex1		1583.6205	1583.636	9.79	43.58
21.75		Hex3HexNAc4 DHex1		1583.6205	1583.632	7.26	0.50
22.74	Man5	Hex5HexNAc2		1355.5095	1355.512	1.84	1.27
23.61	G1F-GlcNAc	Hex4HexNAc3 DHex1		1542.5939	1542.597	2.01	1.03
25.74	(1,6)G1F	Hex4HexNAc4 DHex1		1745.6733	1745.593	-46.00	30.54
26.40	(1,3)G1F	Hex4HexNAc4 DHex1		1745.6733	1745.628	-25.95	10.79
28.85	G1F-GlcNAc +NeuAc1	Hex4HexNAc3 DHex1NANA1		1833.6893	1833.834	78.91	0.20
30.34	G2F	Hex5HexNAc4 DHex1		1907.7261	1907.715	-5.82	7.71

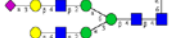
Rituxan							
RT (min)	Short name	Composition	Structura scheme	Expected mass (Da)	Observed mass (Da)	Δmass (ppm)	FLR Area%
32.86	G2F+ NeuAc1	Hex5HexNAc4 DHex1NeuAc1		2198.8215	2198.805	-7.50	1.01
35.70	G2F+ NeuAc2	Hex5HexNAc4 DHex1NeuAc2		2489.9169	2489.917	0.04	0.41

Table S3. Data collection and refinement statistics for the anti-CD20 Fc fragment*

	Anti-CD20 Fc fragment (PDB: 5IW3)	Anti-CD20 Fc fragment (PDB: 5IW6)
Data collection		
Wavelength	0.97915	0.97915
Space group	$C222_1$	$P2_12_12_1$
Cell dimensions		
a, b, c (Å)	64.16, 143.10, 56.56	49.45, 80.00, 139.32
α, β, γ (°)	90.0, 90.0, 90.0	90.00, 90.00, 90.00
Resolution (Å) [†]	50.0–2.05 (2.09–2.05)	50.0–2.34 (2.38–2.34)
R_{sym} (%)	7.6 (37.2)	8.7 (57.1)
I/σ	14.0 (2.9)	32.1 (2.1)
Completeness (%)	98.1 (82.6)	99.9 (100.0)
Total No. of reflections	132524	677459
Unique reflections	17005	24182
Redundancy	3.6 (3.6)	6.8 (6.3)
Refinement		
Resolution (Å)	50.0–2.05 (2.10–2.05)	50.0–2.34 (2.40–2.34)
No. of reflections	15767 (1095)	22794 (1606)
$R_{\text{work}}/R_{\text{free}}$ (%)	18.9/20.7 (24.1/24.3)	22.4/25.9 (31.9/32.9)
No. of atoms		
Protein	1720	3379
Ligand/ion	23	0
Water	245	107
B -factors (Å ²)		
Protein	26.89	60.75
Ligand/ion	37.30	0
Water	40.40	51.22
RMSDs		
Bond lengths (Å)	0.009	0.010
Bond angles (°)	1.44	1.47
Ramachandran Plot (%) [‡]	95.0/5.0/0/0	91.8/7.7/0.6/0

*Three crystallization experiments were performed for each structure. [†]Statistics for the highest resolution shell.

$R_{\text{sym}} = \sum_h \sum_i |I_{h,i} - I_h| / \sum_h \sum_i I_{h,i}$, where I_h is the mean intensity of the i th observation of the symmetry-related reflections of h .

[‡]Residues in the most favoured, additional allowed, generously allowed, and disallowed regions of the Ramachandran plot.

Table S4. Binding affinity of the recombinant anti-CD20 mAb for human Fc γ RIIIa.

	158Val/Phe	K_a (1/Ms)	K_d (1/s)	K_D (M)
Rituxan	Val	4.6×10^4	4.3×10^{-2}	$9.4 \pm 0.02 \times 10^{-7}$
Recombinant mAb	Val	1.7×10^5	1.0×10^{-2}	$5.9 \pm 0.01 \times 10^{-8}$
Rituxan	Phe	2.5×10^4	1.7×10^{-1}	$6.8 \pm 0.02 \times 10^{-6}$
Recombinant mAb	Phe	2.1×10^5	2.7×10^{-2}	$1.3 \pm 0.02 \times 10^{-7}$

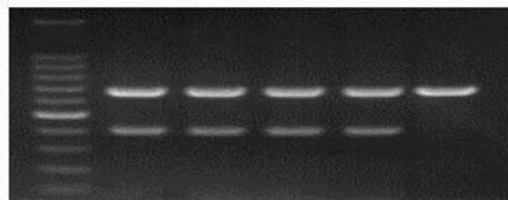
Figure S1

a



b

Marker 1231 1232 0216 0220 WT



c



d

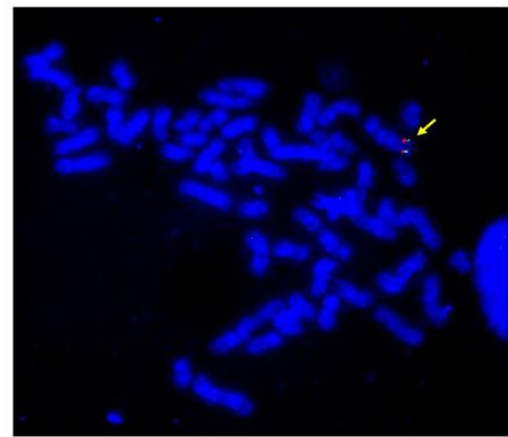


Figure S2

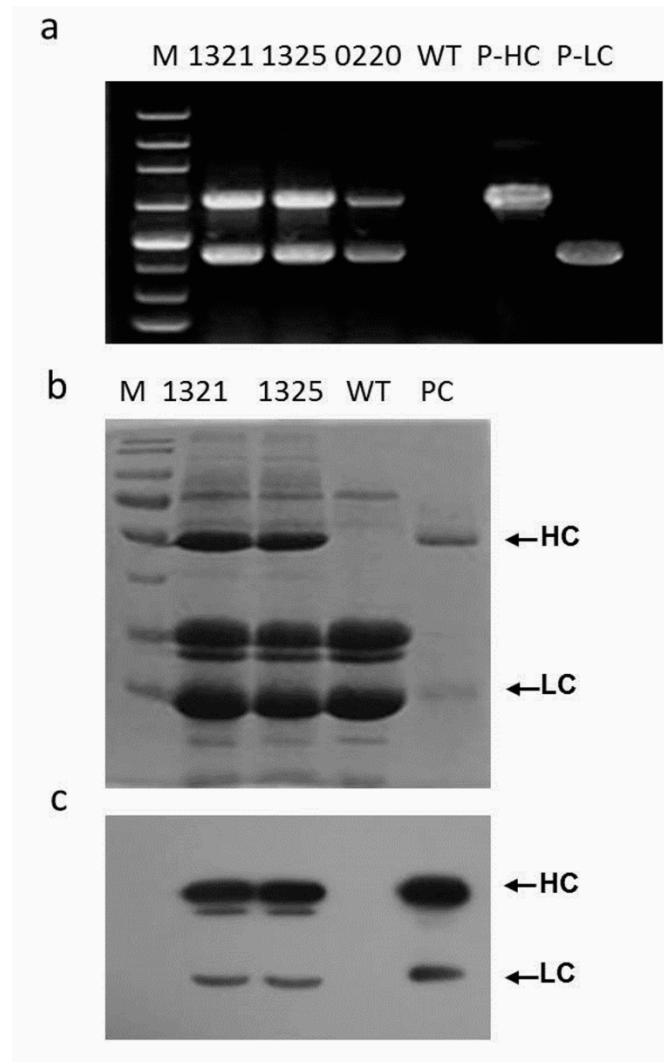


Figure S3

N-terminus

1 QVQLQQPGAE LVKPGASVKM SCKASGYTFT SYNMHWVKQT PGRGLEWIGA
51 IYPGNGDTSY NQKFKGKATL TADKSSSTAY MQLSSLTSED SAVYYCARST
101 YYGGDWYFNV WGAGTTVTVS AASTKGPSVF PLAPSSKSTS GGTAALGCLV
151 KDYFPEPVTV SWNSGALTSG VHTFPAVLQS SGLYSLSSVV TVPSSLGTQ
201 TYICNVNHPK SNKVDKKAE PKSCDKTHTC PPCPAPELLG GPSVFLFPPK

RVE

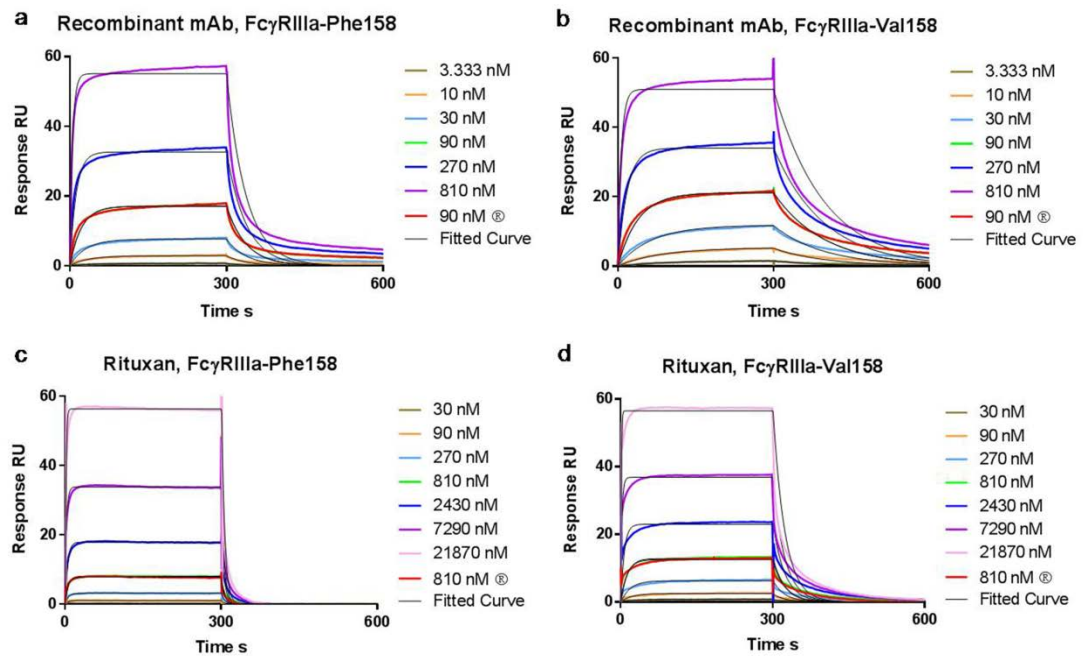
251 PKDTLMISRT PEVTCVVVDV SHEDPEVKFN WYVDGVEVHN AKTKPREEQY
301 NSTYRVVSVL TVLHQDWLNG KEYKCKVSNK ALPAPIEKTI SKAKGQPREP
351 QVYTLPPSRD ELTKNQVSLT CLVKGFYPSD IAVEWESNGQ PENNYKTPP

E EM

401 VLDSDGSSFL YSKLTVDKSR WQQGNVFSCS VMHEALHNHY TQKSLSLSPG
451 K

C-terminus

Figure S4



Full-length gels and blots for SDS-PAGE and Western blotting experiments.

Figure 1(d)

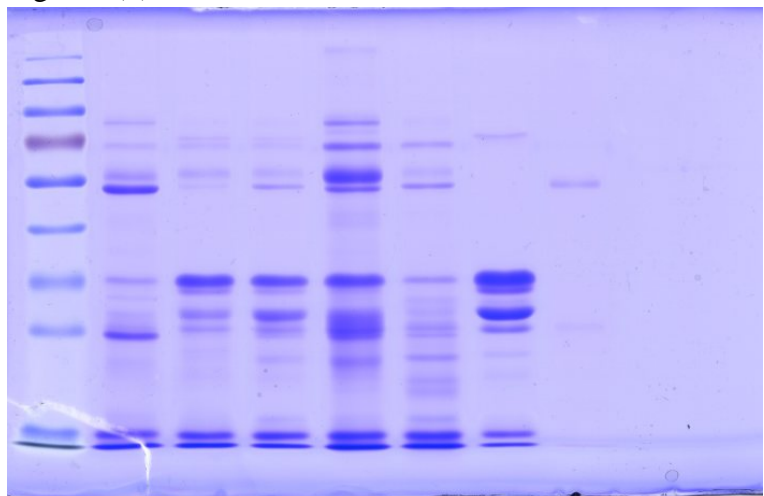


Figure 1(e)

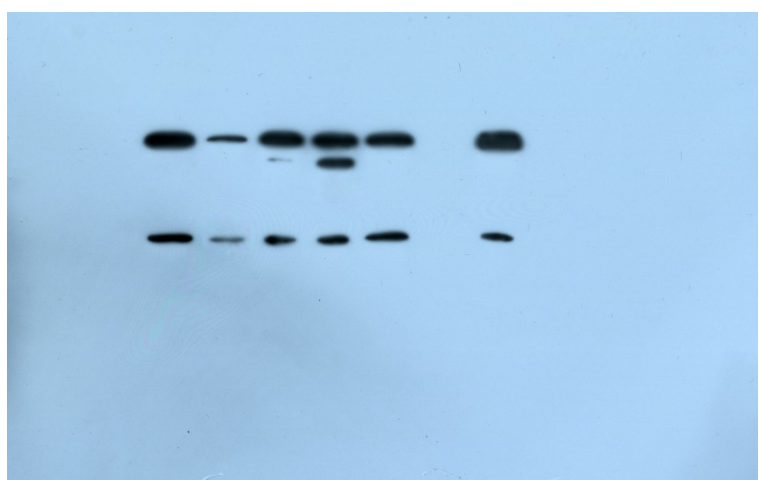


Figure 1(f)

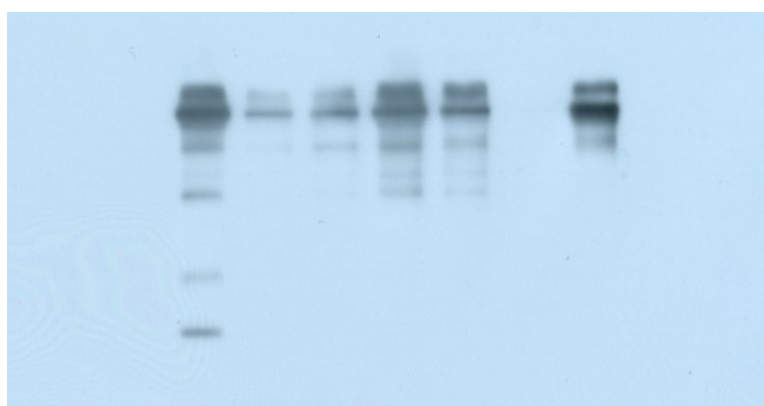


Figure 2(c)

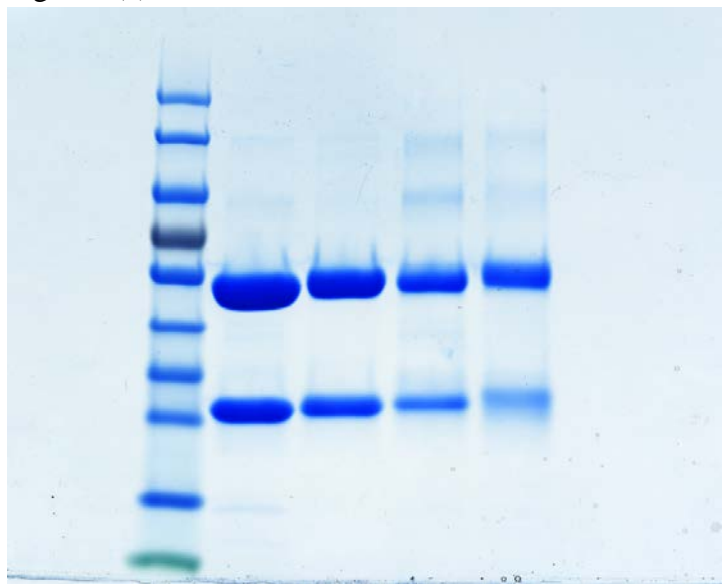


Figure 2(d)

